J9.4 A WIND-PARTITIONING ANALYSIS OF THE ROLE OF EVAPORATION AND HORIZONTAL MOISTURE ADVECTION IN THE ONSET AND EVOLUTION OF THE MJO

Ángel F. Adames-Corraliza*[1], Jérôme Patoux[1] and Ralph C. Foster[2]
1. Department of Atmospheric Sciences, University of Washington, Seattle, WA
2. Applied Physics Laboratory, University of Washington, Seattle, WA.

1. INTRODUCTON

The Madden-Julian oscillation is the dominant component of intraseasonal variability in the tropical atmosphere. It is characterized by eastward-propagating convective centers and associated baroclinic oscillations in the tropical wind field. These anomalies propagate eastward at an average speed of 5 ms^{-1} across the equatorial Indian and western/central Pacific oceans, with a period of roughly 30-90 days (Zhang 2005). Because of its extensive interactions with other components of the climate system and its modulation of the global circulation, the MJO has been the subject of intense study. However, there remain many gaps in our understanding of its initiation and propagation. A reason for current deficiencies in modeling can be attributed to an inadequate understanding of the interactions of the multiple spatiotemporal scales of organized tropical convection (Khouider et al., 2011).

Results from numerous studies show that convectively coupled equatorial waves (CCEWs) interact strongly with the MJO via refinement of its vertical structure, multi-cloud progression, multi-scale convective processes and altering its propagation (Majda and Stechmann, 2011). In particular, equatorial Rossby and Kelvin waves may play a fundamental role in the dynamical structure of the MJO. A potential key feature in understanding the MJO's complexity lies in understanding the role of different wave modes on the momentum and moisture budgets of the MJO. A recent study by Yasunaga and Mapes (2012) suggests that stratiform precipitation is more characteristic of divergent waves (i.e. Kelvin and Inertio-gravity) while small convective systems and pronounced modulation of precipitable water is more characteristic of rotational waves (i.e. Rossby and mixed-Rossby gravity).

Additionally, preliminary results from the joint field campaigns Dynamics of the Madden Julian Oscillation (DYNAMO) and the Atmospheric Radiation Measurement program's (ARM) MJO Investigation Experiment (AMIE) show that the structure of the MJO varies in each individual event. Fig. 1 shows zonal winds obtained at Gan Island during the observation period of AMIE. MJO events were observed during late October, November and December[i]. The strength, duration and vertical structure of the westerly winds associated with the MJO varied significantly with each individual event. Additionally, vertically propagating structures are seen in each event. These results suggest that waves have distinct roles within an active MJO envelope and may be fundamental to its initiation and slow propagation.

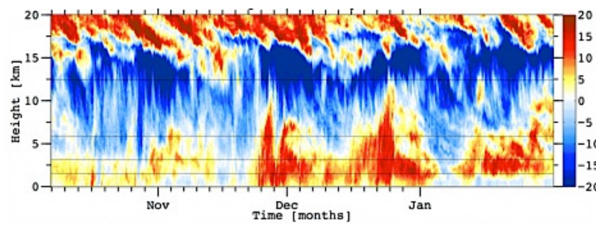

Figure 1. Zonal wind (in m/s, filled contours) measured from soundings at the ARM site at Gan Island from October 1, 2011 – February 8, 2012. Black lines denote pressure levels of 850, 700, 500 and 200 hPa, from bottom to top. Data obtained from the ARM program database.

In this study, we evaluate the contribution of flow emerging from vorticity and divergence elements to the advection of moisture within the boundary layer (BL) and lower free troposphere during MJO events. For this purpose, we make use of the four times daily data from the ERA-Interim dataset from 1979-2011 gridded on pressure surfaces with a resolution of 1.5°.

2. THE WIND PARTITIONING TECHNIQUE

Equatorially trapped wave solutions using inviscid shallow water equations (Matsuno 1966) not only describe the propagation characteristics of each mode, but can also show whether a mode is predominantly rotational or divergent. We could take advantage of these properties by partitioning the wind field in the tropical region into its irrotational, non-divergent and background components using the method developed by Bishop (1996) and adapt it to a tropical channel grid with a latitudinal extent of 30°S-30°N. The method consists of identifying the local flow with elements of vorticity and divergence, and attributing the corresponding wind field to it. The technique is briefly described below for the non-divergent component of the flow and the reader is referred to Bishop (1996) for a more complete derivation.

We index a grid by $1 < k < M - 1$ along the x-coordinate and $1 < l < N - 1$ along the y-coordinate. A vorticity element, C_{kl}, centered at (x', y') contributes to the wind at any point (x,y). By adding all the contributions from vorticity elements throughout the grid, one reconstructs the total non-divergent wind field induced at (x, y):

---

* *Corresponding author address:* Ángel F. Adames-Corraliza, Department of Atmospheric Sciences, University of Washington, ATG Building Box 351640 Seattle, WA 98195-1640. email:

[i] It can be debated whether the MJO event observed in December 2011 was a distinct event or a redevelopment of the previous MJO.

$$u_\psi = \frac{1}{2\pi} \sum_{k=1}^{M-1} \sum_{l=1}^{N-1} C_{kl} \frac{-(y - y'_{kl})}{r_{kl}^2} \quad (1a)$$

$$v_\psi = \frac{1}{2\pi} \sum_{k=1}^{M-1} \sum_{l=1}^{N-1} C_{kl} \frac{(x - x'_{kl})}{r_{kl}^2} \quad (1b)$$

where r_{kl} is the distance between (x,y) and each vorticity element C_{kl}. Similarly the sum of the contributions from a discrete divergence element will yield the irrotational component of the wind field. The remaining component $\vec{u}_\theta = \vec{u} - (\vec{u}_\psi + \vec{u}_\chi)$ is irrotational and non-divergent, and is induced by vorticity and divergence elements outside the partitioned domain. It thus represents the "background" wind, or "environmental" wind and can be regarded as a "laterally forced" velocity.

Fig. 2 shows a composite of $\vec{u}_\psi$ (top) and $\vec{u}_\chi$ (bottom) with humidity anomalies overlayed for MJO phase 6 (Wheeler and Hendon, 2004). The strongest humidity anomalies are associated with a Rossby gyre located northwest of Australia. A broader, yet weaker anomaly, located further east, is closely associated with convergence. A suppressed phase is clearly seen in the Indian Ocean with negative anomalies closely in phase with lower tropospheric divergence. The suppression progresses slightly behind the westerly winds associated with the Rossby gyres. Thus it appears that the partition correctly captures the Kelvin (irrotational) and Rossby (non-divergent) components of the MJO, with the Kelvin portion leading the Rossby component.

The background component of the wind field is shown in Fig. 3. A broad area of weak winds is observed in the figure, with a maximum of near 1 ms^{-1} observed over the western Pacific. The flow corresponds well to geopotential anomalies outside the partition region, with westerlies associated with cyclonic flow and easterlies associated with anti-cyclonic flow. It is unclear at this point of our research whether the advection of moisture by the background flow has any significance.

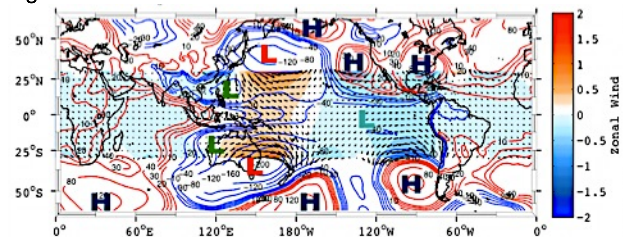

Figure 3. The background flow component for MJO phase 6. Full winds are represented in arrows while its zonal wind component is color contoured. Blue contours denote negative geopotential anomalies (troughing) while red contours denote positive geopotential anomalies (ridges). Contour lines begin at intervals of 10 m^2s^{-2} and increase at invervals of 40 m^2s^{-2} after 40 m^2s^{-2} in order to show some details of geopotential changes in the tropics. Mean and seasonal trends are removed for each variable. Red L's represent centers of low pressure outside the partitioned domain, the cyan L roughly locates the low pressure center associated with the Kelvin component of the MJO, while the green L's represent the lows associated with the Rossby gyres. H's denote areas of anomalous ridging.

3. The Moisture budget of the MJO

The wind partitioning technique can be further applied to study the moisture budget of the MJO. The moisture (q) tendency equation for intraseasonal anomalies is defined as (Hsu and Li, 2012):

$$\frac{\partial q'}{\partial t} = -(\vec{u} \cdot \nabla q)' - (q \nabla \cdot \vec{u})' - \frac{\partial (\omega q)'}{\partial p} + \frac{Q'}{L} \quad (2)$$

where the terms on the right hand side represent the intraseasonal contributions of horizontal advection, moisture convergence, vertical moisture flux and evaporation/condensation, respectively. We will focus on the contribution of horizontal advection, which can be broken down into the partitioned components:

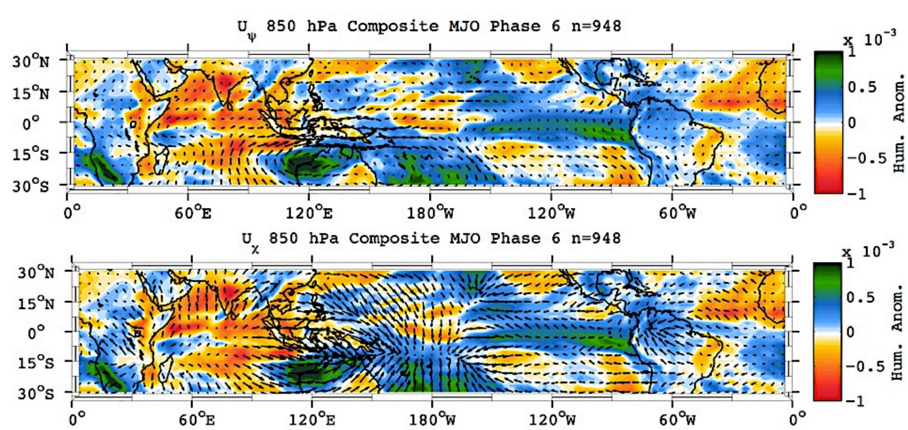

Figure 2. Irrotational (top) and nondivergent (bottom) components of the wind field (arrows) composited for MJO phase 6 during boreal winter. Colored contours denote humidity anomalies (fraction of humidity per kg of air). For each variable the mean and seasonal trends were removed.

$$\vec{u} \cdot \nabla q = \left(\vec{u}_\psi + \vec{u}_\chi + \vec{u}_\theta\right) \cdot \nabla q \qquad (3)$$

Thus, we can evaluate separately the contribution of rotation, divergence, and the environment on the advection of moisture on the MJO.

Advection of moisture by each component was calculated for each vertical level and integrated for the BL and lower free troposphere. The limits of the BL and lower free troposphere were selected to be 1000-850 hPa and 850-500 hPa, respectively. Integration for the BL was done using the following equation:

$$(\vec{u} \cdot \nabla q)_{BL} = \frac{1}{g}\int_{1000\ hPa}^{850\ hPa} \vec{u} \cdot \nabla q \ dp \qquad (4)$$

The same is done for the free troposphere using its respective integration limits. Results using integrated advection are presented in the following section.

4. REGRESSION PLOTS

Lag composite plots are done based on MJO filtered OLR data (eastward zonal wavenumbers 1-10 and periods of 25-80 days). The method used is similar to that employed by MacRitchie and Roundy (2012). The mean and seasonal cycles of advection are removed, and the obtained anomalies are co-located to the filtered OLR anomalies. Results are averaged from latitudes 10°S-10°N, and for every longitude from 60°-120° (in increments of 2.5°, for a total of 25 points). Fig. 4 shows a composite of total advection for the BL (1000-850 hPa) and free troposphere (850-500 hPa). Positive tendencies in the BL are seem to lead tendencies in the free troposphere and propagate at a different speed. It is also worth noticing that free troposphere advection is stronger than BL advection by a factor of six (note the different color scales).

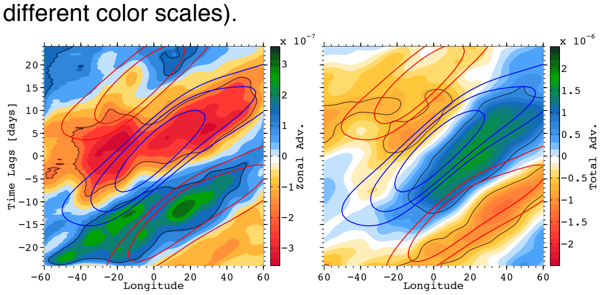

Figure 4. BL (1000-850 hPa, left) and free troposphere (850-500 hPa, right) moisture advection for the full wind field component. Blue contours denote negative OLR anomalies while red contours denote positive OLR anomalies and are shaded every 3 Wm^{-2} beginning at 3 Wm^{-2}. Black contours correspond to one standard deviation in the regressed advection anomalies.

4.1 Contribution of non-divergent advection

Fig. 5 shows a lag composite for the zonal and meridional advections from non-divergent elements. For the BL, it appears that zonal advection is the predominant mechanism early on during an MJO, while meridional advection dominates once convection strengthens. Additionally, zonal advection slightly leads meridional advection in these plots. This would correspond to Rossby gyres advecting dry air from higher latitudes and then advecting it zonally through westerly winds. For the moistening case, it would correspond to easterly winds advecting moist air while the drier air is being pushed away towards higher latitudes. The free troposphere case is more complex. While meridional advection is similar to that in the BL, zonal advection appears different. It first appears nearly in phase with the convective activity but begins to lag it once the anomaly strengthens. It is unknown why this would happen, but it might be due to a change in the vertical moisture profile of the MJO as it progresses, or signal a distinct difference between developing and mature phases of the MJO.

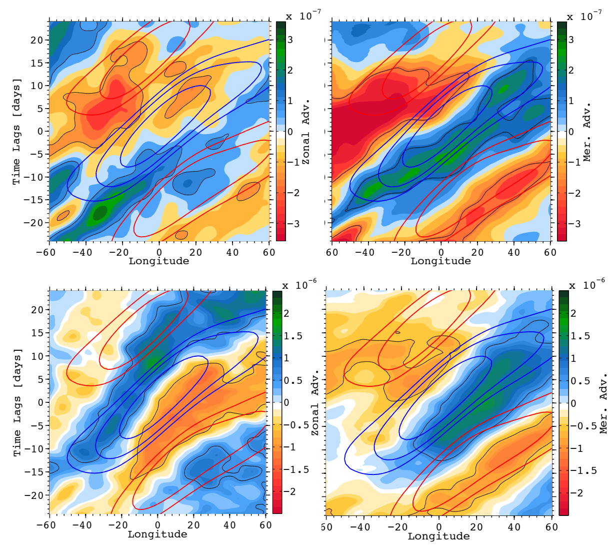

Figure 5. Zonal (upper left) and meridional (upper right) advection for the non-divergent component of the flow within the BL. Lower panels show the same but for free troposphere.

4.2 Contribution of irrotational advection

The contribution from divergence elements on the moisture budget of the MJO is shown in Fig. 6. It is observed to be significantly weaker than the non-divergent advection and lies nearly opposite in phase with the enhanced convection of the MJO. This is because, once a convective envelope is established, the irrotational winds will point up the moisture gradient, leading to negative advection ($-\vec{u}_\chi \cdot \nabla q < 0$) . We remark that the irrotational component also affects the moisture budget through the second and third terms in equation (2), which are positive and are larger than the advection component (Hsu and Li, 2012). Finally, as in the case of the non-divergent component, meridional advection is the stronger of the two components. Advection in the free troposphere (not shown) is similar to that observed in the BL, though stronger.

4.3 Contribution of background advection

The contribution of vorticity and divergence elements from latitudes higher than 30° are much weaker than the local elements of vorticity and divergence, with the exception of zonal advection in the lower free troposphere. Fig. 7 shows

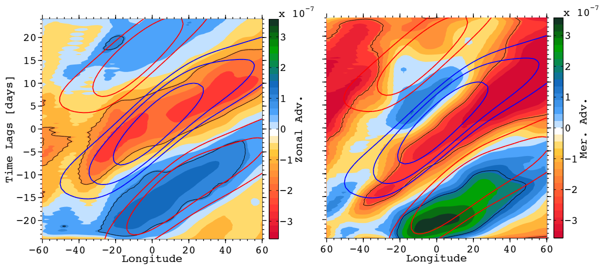

Figure 6. Similar to 5 but for the irrotational component of the wind field. Only the BL component is shown.

that significant positive zonal advection is ahead of the MJO envelope while drying slightly lags the convective center. The same is not observed for meridional advection, where advection is much weaker and a pattern is difficult to observe.

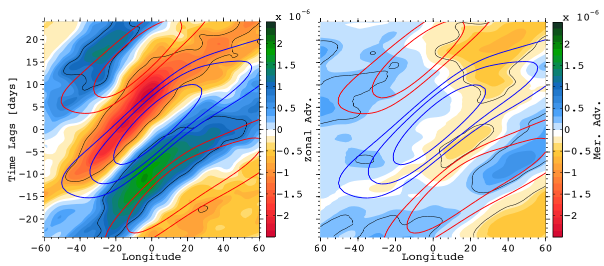

Figure 7. Similar to 5 but for the background component of the wind field. Only the free troposphere component is shown.

5. DISCUSSION AND CONCLUSIONS

In general, moisture advection in the lower free troposphere is stronger than advection within the BL. However, advection by each wind component is different in both layers. In particular, the background flow, which we interpret as flow associated with the extratropics, appears to have a significant role in the moisture budget of the MJO in the free troposphere while only having a minor role in the BL. It also appears that meridional advection by vorticity elements plays a significant role in moistening the environment ahead of convection. The only component that had similar behavior in both layers (zonally and meridionally) was the irrotational component, which acts to dry out the MJO envelope.

Results in Fig. 4 do not show anything unexpected, positive advection leads the MJO signal while significant drying lags the anomaly. However, it is shown that the total advection profile observed is a result of a continuous interaction of vorticity and divergence elements. Once extracted and studied individually, one finds that winds associated with vorticity elements contribute to the advection of moisture in a way different than those that emanate from divergence elements. These findings could have important implications for individual MJO events. For example, events that have strong westerly wind bursts (as was the November 2011 case) might have a moisture advection profile more similar to Fig. 5 than cases in which the westerlies are not as strong. Because of the potential of modifying the moisture tendencies of an intraseasonal oscillation, and thus altering its structure and propagation, the effect of rotating and divergent elements within an MJO envelope warrants further study. Additionally, the contribution of lateral sources to maintaining or enhancing moisture ahead of the MJO envelope merits some attention.

Future work includes partitioning each wind component into low and high frequency contributions and study the role of moisture advection from higher frequency waves in relation to the lower-frequency MJO.

ACKNOWLEDGMENTS

This work is supported by the National Science Foundation Graduate Fellowship Program (NSF-GRFP) grant DGE – 0718124 and NASA – OVWST grant # NNX10AO87G. Data was obtained from ECMWF's ERA-Interim dataset.

REFERENCES

Bishop C. H., 1996: Domain independent attribution. I: Reconstructing the wind from estimates of vorticity and divergence using free space Green's functions. *J. Atmos. Sci.*, **53**, 241–252.

Hsu, P. and Li, T., 2012: Role of the BL Moisture Asymmetry in Causing the Eastward Propagation of the Madden-Julian Oscillation. *J. Clim.*, In Press.

Khouider B., Y. Han, A. J. Majda and S. N. Stechmann, 2011: Multiscale Waves in an MJO Background and Convective Momentum Transport Feedback. *J. Atmos. Sci.*, **69**(3), 915–933.

MacRitchie, K., P. E. Roundy, 2012: Potential Vorticity Accumulation Following Atmospheric Kelvin Waves in the Active Convective Region of the MJO. *J. Atmos. Sci.*, **69**, 908–914.

Majda A. J. and S. N. Stechmann, 2011: Multi-scale theories for the MJO. *Intraseasonal Variability of the AtmosphereOcean Climate System*, W. K. M. Lau and D. E. Waliser, **2**, 20.

Matsuno T., 1966: Quasi-geostrophic motions in the equatorial area. *J. Met. Soc. Jap.*, **44**, 2543.

Yasunaga K. and B. Mapes, 2012: Differences between More Divergent and More Rotational Types of Convectively Coupled Equatorial Waves. Part I: Space-Time Spectral Analyses. *J. Atmos. Sci.*, **69**(1), 3–16.

Wheeler, M,and H. H. Hendon, 2004: An all-season real-time multivariate MJO index: Development of an index for monitoring and prediction. *Mon. Wea. Rev.*, **132**, 1917–1932.

Zhang C., 2005: Madden-Julian Oscillation. *Rev. Geophys.*, **RG2003**